CRISPR-Cas is beneficial in plasmid competition, but limited by competitor toxin-antitoxin activity when horizontally transferred.

David Sünderhauf*[1], Jahn R. Ringger[1+], Leighton James Payne[2], Rafael Pinilla-Redondo[2], William H. Gaze[3], Sam P Brown[4, 5], Stineke van Houte*[1]

*corresponding authors; DS: david@sunderhauf.net, SvH: C.van-Houte@exeter.ac.uk

[1] Environment and Sustainability Institute, University of Exeter Penryn Campus, Penryn, TR10 9FE, UK

[2] Section of Microbiology, Department of Biology, University of Copenhagen, Copenhagen, Denmark

[3] European Centre for Environment and Human Health, University of Exeter Penryn Campus, Penryn, TR10 9FE

[4] School of Biological Sciences, Georgia Institute of Technology, Atlanta, Georgia, USA

[5] Center for Microbial Dynamics and Infection, Georgia Institute of Technology, Atlanta, Georgia, USA

[+]current address: Department of Environmental Sciences, University of Basel, 4051 Basel, Switzerland

ORCIDs:

DS - 0000-0002-8007-3351; JR - 0009-0002-1831-3630; LJP - 0000-0003-2305-6827; RPR - 0000-0003-3521-460X; WHG - 0000-0002-9345-6204; SPB - 0000-0003-1892-9275; SVH - 0000-0001-7047-1308

Abstract

Bacteria can encode dozens of different immune systems that protect cells from infection by mobile genetic elements (MGEs). Interestingly, MGEs may also carry immune systems, such as CRISPR-Cas, to target competitor MGEs, but it is unclear when this is favoured by natural selection. Here, we develop and test novel theory to analyse the outcome of competition between plasmids when one carries a CRISPR-Cas system that targets the other plasmid. Our model and experiments reveal that plasmid-borne CRISPR-Cas is beneficial to the plasmid carrying it when the plasmid remains in its host. However, CRISPR-Cas is selected against when the plasmid carrying it transfers horizontally, if the competitor plasmid encodes a toxin-antitoxin (TA) system that elicits post-segregational killing. Consistent with a TA barrier to plasmid-borne CRISPR-Cas, a bioinformatic analysis reveals that naturally occurring CRISPR-Cas-bearing plasmids avoid targeting other plasmids with TA systems.

Our work shows how the benefit of plasmid-borne CRISPR-Cas is severely reduced against TA-encoding competitor plasmids, but only when plasmid-borne CRISPR-Cas is horizontally transferred. These findings have key implications for the distribution of prokaryotic defenses and our understanding of their role in competition between MGEs, and the utility of CRISPR-Cas as a tool to remove plasmids from pathogenic bacteria.

Introduction

Mobile genetic elements (MGEs) are widely distributed throughout the prokaryotic tree of life. As facilitators of horizontal gene transfer, MGEs have the potential to shape ecology and evolution of bacterial populations and to disseminate genes, such as antimicrobial resistance (AMR) genes, between bacterial strains and species. Conjugative plasmids are the most effective distributors of horizontally transferred genes in bacterial communities (Nazarian *et al.*, 2018), and are therefore key drivers of the AMR crisis. Plasmids frequently co-infect the same bacterial cell (San Millan *et al.*, 2014), and therefore often compete for the same ecological niche, i.e. their bacterial host. Prokaryotic immune systems are abundant throughout bacterial genomes and can alter not only how the bacterial host interacts with MGEs, but also how co-infecting MGEs interact with each other (Rocha and Bikard, 2022). Indeed, immune systems are more frequently carried by MGEs than by bacterial chromosomes (reviewed in (Beamud *et al.*, 2024)). However, how natural selection acts on immune systems when they are encoded on chromosomes versus on MGEs is an open question.

CRISPR-Cas (Clustered Regularly Interspaced Short Palindromic Repeats – CRISPR-associated) is an adaptive prokaryotic immune response, where an immune memory is formed by integrating a short sequence of an invading MGE into the CRISPR locus as a “spacer”. This array of spacers is expressed and processed into small guide RNA that associate with a Cas protein or protein complex. Together, this ribonucleoprotein complex acts as an RNA-guided DNA or RNA nuclease to specifically recognise the MGE during a subsequent infection, and cleave its genome and/or transcripts (reviewed in (Makarova *et al.*, 2020)). CRISPR-Cas systems are common on bacterial chromosomes (~42% of chromosomes carry a CRISPR-Cas

system), but are also found on ~3% of plasmids. (Pinilla-Redondo *et al.*, 2022). Plasmid-borne CRISPR-Cas systems can be nucleolytic or silence gene expression, and have been implicated in plasmid warfare (reviewed in (Koonin and Makarova, 2024)): plasmids' CRISPR spacers tend to match other, competing plasmids – particularly those of similar size which occupy the same niche (Pinilla-Redondo *et al.*, 2022; Benz *et al.*, 2024).

In response, plasmids may invest in traits that give them a fitness advantage in the face of such competition with CRISPR-Cas-bearing plasmids. These can be either through direct interference with CRISPR-Cas such as anti-CRISPRs (Mahendra *et al.*, 2020), or through other, CRISPR-Cas-independent, features such as plasmid incompatibility (Novick, 1987), Bet/Exo systems (Roy *et al.*, 2020), entry exclusion (Garcillán-Barcia and de la Cruz, 2008), and toxin-antitoxin (TA) systems (Harms *et al.*, 2018). Of these, TA systems are highly prevalent across plasmids: together with multimer resolution systems and partition systems, TA were theorised to be essential to large virulence plasmids (Sengupta and Austin, 2011) and a recent analysis of over 40000 NCBI-deposited plasmids of varying sizes found that 35% encoded at least one TA locus (Guan *et al.*, 2024). TA systems function by simultaneous production of a toxin and a short-lived antitoxin. If the plasmid – and therefore the TA genes it carries – are removed, the antitoxin will degrade faster than the toxin, freeing the toxin up to harm or kill the bacterial host. This addictive nature of TA systems means their removal is strongly selected against (Harms *et al.*, 2018), and this phenomenon is theorised to be beneficial to plasmid competition (Cooper and Heinemann, 2000; Cooper *et al.*, 2010; Rankin *et al.*, 2012). Previous work has shown that TA systems may also interfere with CRISPR-Cas targeting of plasmids: A chromosomally-encoded Type I-E CRISPR-Cas system was shown to be selected against when it targeted a CcdAB TA-

encoding plasmid (Van Sluijs *et al.*, 2019), and pOXA-48a's pemIK TA system was identified as a barrier to removal by a mobilisable plasmid encoding a synthetic Type II CRISPR-Cas9 system (Reuter *et al.*, 2021).

While it is therefore clear that both TA systems and CRISPR-Cas immune systems are important during within-cell plasmid competition (Rankin *et al.*, 2012; Benz *et al.*, 2024), it is unclear how selection acts on these traits when they directly compete with one another. Given that CRISPR-Cas-directed removal of TA plasmids is selected against (Van Sluijs *et al.*, 2019; Reuter *et al.*, 2021), we hypothesize that the benefit of CRISPR-Cas systems to plasmid competition may be limited by the presence of a TA system on competing plasmids.

To explore this hypothesis, we constructed a mathematical model predicting the outcome of plasmid competition between a TA-bearing and a CRISPR-Cas-bearing plasmid within an individual host, dependent on whether the CRISPR-Cas plasmid was acting offensively (i.e. the CRISPR-Cas-bearing plasmid invaded the host) or defensively (i.e. the CRISPR-Cas-bearing plasmid protected its host from competitor plasmid invasion). The model predicted that the outcome of plasmid competition depended on this ecological scenario, as well as TA and CRISPR-Cas strength: when offensive, CRISPR-Cas provided diminishing benefits to its plasmid when faced with a stronger competing TA system that was already established in the host cell. We further built an experimental system by allowing IncP plasmids pKJK5::csg (IncP1ε; CRISPR-Cas9 plasmid) and RP4 (IncP1α; TA plasmid) to compete for *E. coli* hosts. We found that carrying active CRISPR-Cas was always beneficial to pKJK5 when CRISPR-Cas was acting defensively. By contrast, selection only favoured

120 CRISPR-Cas on pKJK5 during offense (i.e. when invading a host in which RP4 was
121 established) if the competitor RP4 did not carry an active TA system. Finally, we further
122 tested our theory and generalized our experimental results by bioinformatically
123 analysing plasmids carrying CRISPR-Cas systems and their target plasmids and
124 found that these targeted plasmids did not typically encode TA systems.

125 This work highlights the limits of an active CRISPR-Cas immune system in plasmid
126 competition and underlines the advantages of TA systems to plasmid spread and
127 persistence.

128 **Results**

129 Mathematical modelling predicts that CRISPR-Cas benefit is dependent on TA activity
130 of competitor plasmids.

131 Both CRISPR-Cas and toxin-antitoxin systems have been implicated in plasmid-level
132 competition (Rankin *et al.*, 2012; Benz *et al.*, 2024). In a mathematical analysis, we
133 set out to formalise the relative benefits of CRISPR-Cas to a plasmid when competing
134 with a plasmid encoding TA, depending on asymmetries due to distinct offensive
135 versus defensive roles of CRISPR-Cas and TA. A defensive role occurs when a
136 plasmid is already resident in a cell line. In contrast, an offensive role occurs when a
137 plasmid is a newly arrived invader in a cell (i.e. the plasmid is horizontally transferred
138 to a new host).

139 To formalise plasmid competition dynamics, we begin with a simple conceptualisation
140 of plasmid competition (Figure 1A). Our approach focuses on cells co-infected with
141 both plasmids (*CT* and *TC* cells), with plasmids differentiated by their order of arrival.
142 *C* represents cells where a CRISPR-Cas plasmid is resident, while *T* represents cells
143 where a TA plasmid is resident. In the event *C* cells experience a conjugation event
144 introducing a TA-plasmid, we have a *CT* cell containing both a resident CRISPR-Cas
145 plasmid and an invading TA plasmid. Conversely, *TC* cells are created when a *T* cell
146 acquires a CRISPR-Cas plasmid.

147 Our model defines transition rates from co-infected states (*CT* or *TC*) to singly infected
148 states (*C* or *T*) (arrows in Figure 1A, more detail in Figure S1A). These transition rates
149 are defined by plasmid segregational loss (baseline rate s), modified by *C*- and *T*-
150 specific traits of CRISPR-Cas-induced enhanced segregation (blue in Figure 1A;
151 multiplicative factor x; $x > 1$ implies increased segregation rate $x \cdot s$) and TA-induced

152 post-segregational killing (red arrow in Figure 1A; probability of PSK y). In the event
153 of PSK, we assume that the liberated resources (nutrients, space) can enhance the
154 growth of remaining C or T cells, weighted by parameter f (Rankin *et al.*, 2012). Finally,
155 asymmetries in parameter values between resident and invader roles are captured by
156 subscripts r and i. Given lower plasmid copy number and lower gene expression for
157 invading versus established plasmids (Fraikin *et al.*, 2024), our default assumptions
158 are $s_i > s_r$; $x_r > x_i \geq 1$; $1 > y_r > y_i \geq 0$. Given spatial structuring so that T cells are enriched
159 in neighbourhood of TC cells (and vice-versa for C near CT cells), we further assume
160 $1 > f_r + f_i > f_r > f_i \geq 0$. The resulting transition rates (Figure S1A, equations E1-E4) are
161 used to define fitness functions for CRISPR-Cas and TA plasmids in both resident and
162 invader contexts (equations E5-8, Supplementary Results 1). Finally, we used these
163 transition rates to calculate the relative competitive success of the CRISPR-Cas
164 plasmid R_C (Figure 1A, equations E9-E10), which is a measure of the relative fitness
165 of the CRISPR-Cas compared to the TA plasmid.

166 Analysis of R_C for either resident or invader CRISPR-Cas plasmids provided the
167 following core predictions concerning the impact of CRISPR-Cas and TA investments
168 (x and y) on their relative competitive success (derivations are detailed in
169 Supplementary Results 1): Firstly, in the absence of PSK (no TA; $y = 0$), increasing
170 investment in CRISPR-Cas (increasing x) always increases CRISPR-Cas competitive
171 success, regardless of whether in a defensive (Figure 1B) or offensive role (Figure
172 1C). Secondly, in the presence of PSK ($y > 0$), increasing CRISPR-Cas investments
173 is still beneficial in a resident context (Figure 1B), but can become detrimental in an
174 offensive role, given sufficiently high resident PSK (y_r) (Figure 1C, strong TA).
175 Analytical conditions for this qualitative shift in behaviour are defined in Supplementary
176 Results 1.

177 In conclusion, our mathematical modelling predicted an asymmetric outcome of
178 plasmid competition, depending on CRISPR-Cas mode of action. When resident,
179 investing in stronger CRISPR-Cas always benefitted its own plasmid. However, in
180 offense CRISPR-Cas switched from an asset to a liability in plasmid competition,
181 dependent on a sufficiently strong TA response on the competitor plasmid.

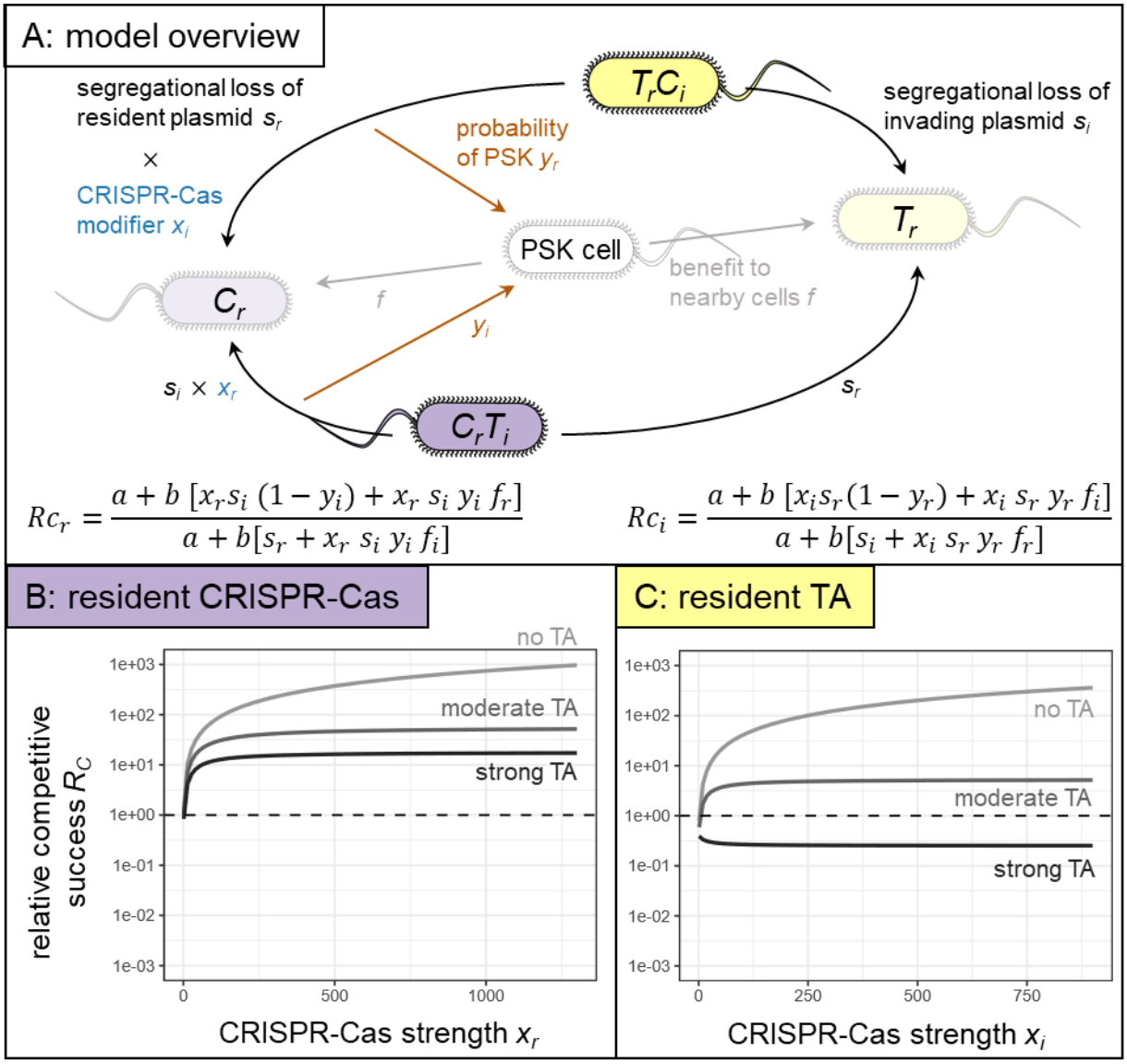

182

183 Figure 1: Mathematical modelling predicts that CRISPR-Cas has a greater potential to
184 benefit its plasmid in defence than in offense.

185 A: Structure of the mathematical model. *C* (CRISPR-Cas bearing) and *T* (TA-bearing)
186 plasmids reside in host cells, and we consider five distinct cell types. *CT* denotes a *C*
187 cell that has been invaded by a *T* plasmid and vice-versa; PSK cells are dead cells
188 after post-segregational killing. When the plasmids co-reside, they are subject to basic
189 biological parameter *s* (segregational loss). CRISPR-Cas and TA alter parameter *s* by
190 their own modes of action *x* and *y* respectively. Parameter *f* describes the positive
191 effect PSK cells have on growth of *T* kin. All parameters adopt distinct values when
192 their respective plasmids are resident (*r*) or invasive (*i*). *a* and *b* refer to baseline
193 plasmid fitness and a scaling parameter of the relevant competitive transition
194 respectively. For full equations, see Supplementary Results 1.

195 B, C Relative competitive success of the *C* plasmid, in either resident (R_{Cr}) or invader
196 role (R_{Ci}). Values >1 describe a CRISPR-Cas plasmid with higher fitness than the TA
197 competitor, and values <1 describe a more competitive TA plasmid as a function of
198 strength of CRISPR-Cas system *x*. This relationship is shown for three example TA
199 strengths *x*. Both *x* and *y* adopt different maximum values depending on which plasmid
200 is resident (no TA y_i / y_r = 0; moderate TA y_i / y_r = 0.33 / 0.66; strong TA y_i / y_r = 0.66 /
201 0.99; maximum x_r = 1300; maximum x_i = 900). This figure presents horizontal cross-
202 sections of the relative competitive success across the entire *x* and *y* parameter space
203 presented in Figure S1B-C. Parameter choices are specified in Supplementary
204 Results 1.

205

206

207

208 Experimentally competing a CRISPR-Cas and TA plasmid showed a universal
209 CRISPR-Cas benefit in defence, but not in offense.

210 Our mathematical modelling predicts that the benefits of a plasmid-encoded CRISPR-
211 Cas system are limited during competition with TA plasmids. We sought to test these
212 predictions experimentally in a model system where we could modulate CRISPR-Cas
213 and TA strength in a binary way by turning these systems on and off. To this end, we
214 used competitor plasmids pKJK5::csg and RP4 as models to examine how selection
215 acts on plasmid-encoded CRISPR-Cas under “defensive” and “offensive” modes of
216 action (Figure 2A-B). Due to plasmid incompatibility resulting in segregational loss,
217 these plasmids cannot be co-maintained in the same host indefinitely but can co-exist
218 for several generations (Bahl *et al.*, 2007), giving ample window of opportunity for
219 plasmid competition within the same bacterial host. Plasmid pKJK5::csg was
220 engineered to carry a minimal Type II CRISPR-Cas9 system (Sünderhauf *et al.*,
221 2023b), and we turned CRISPR-Cas activity on or off by using two isogenic plasmid
222 variants that only differed in their respective fixed targeting specificity (Figure 1A, see
223 Methods). Competitor plasmid RP4 naturally carries the Type II TA system *parABCDE*,
224 where *parABC* form a segregational stability system and *parDE* code for a TA system
225 that can kill plasmid-free segregants (Adamczyk and Jagura-Burdzy, 2003). Due to the
226 higher stability of the ParE DNA gyrase inhibiting toxin over the ParD antitoxin, *parDE*
227 loss causes an arrest in cell division, SOS induction, and cell filamentation (Fraikin
228 and Melderen, 2023). We turned RP4’s TA activity off by supplying an expression
229 vector engineered to carry RP4’s *par* TA operon (pCDF1b_par) to all potential plasmid
230 hosts, thus allowing supply of the antitoxin *in trans* and thereby negating the PSK
231 effect of RP4’s TA system. As a control, empty vector pCDF1b was supplied in all
232 treatments where TA remained turned on (Figure 1A). These vectors pCDF1b and

233 pCDF1b_par are compatible with both pKJK5 and RP4 and were maintained
234 throughout all experiments in the absence of antibiotic selection (Figure S3).

235 To assess plasmid competition outcome under different modes of CRISPR-Cas action,
236 we set up mating assays including three *Escherichia coli* DH5α hosts with different
237 plasmid content (Figure 2B). In this way, we could track plasmid competition when
238 CRISPR-Cas was acting defensively (a pKJK5 host was invaded by RP4) and when
239 CRISPR-Cas was acting offensively (an RP4 host was invaded by pKJK5). Further,
240 we included an intermediate scenario where both plasmids invade an initially naïve,
241 plasmid-free host. In this scenario, the mode of action of CRISPR-Cas could be either
242 offensive or defensive. After solid-surface filter mating, we measured numbers of each
243 host and their respective plasmid content by selective plating, making use of different
244 chromosomal resistance gene tags in each *E. coli* host. We calculated the plasmids'
245 competitive ratio for each scenario. This metric is a log10 of the proportion of pKJK5
246 over RP4 carriage within hosts and describes which plasmid won the competition for
247 each host; positive values indicate that CRISPR-Cas plasmid pKJK5 was more
248 abundant in its host, and negative values indicate that TA plasmid RP4 was more
249 abundant.

250 This analysis revealed that when CRISPR-Cas was acting defensively, the CRISPR-
251 Cas plasmid won the competition in every case where CRISPR-Cas was switched on
252 (Figure 2C; competitive ratio = 1.41 (N=1) and 1.94 ± 0.0085 respectively; significantly
253 higher than 0 with $p < 0.001$ after T-test and Bonferroni adjustment for multiple testing
254 with $\alpha = 0.005$). In stark contrast, when CRISPR-Cas was acting offensively, switching
255 on CRISPR-Cas had a differential effect depending on TA status of the competitor
256 plasmid. When TA was absent from the competitor, switching on CRISPR-Cas brought
257 little or no benefit to CRISPR-Cas plasmid pKJK5 (Figure 2D; competitive ratio = 0.32

258 ± 0.13; p = 0.07 and non-significant with α = 0.005). However, when the competitor
259 plasmid's TA was switched on, switching on CRISPR-Cas was highly detrimental to
260 pKJK5 (competitive ratio = -2.19 ± 0.11; p < 0.001 and significant with α = 0.005).

261 In the naïve host, switching on CRISPR-Cas on its own benefitted pKJK5 (Figure 2E;
262 competitive ratio 0.73 ± 0.1; p = 0.0019 and significant with α = 0.005). When TA was
263 switched on alongside this, there was no clear winner of the competition (competitive
264 ratio = -0.21 ± 0.096; p = 0.1), however CRISPR-Cas still provided a benefit to pKJK5
265 relative to the scenario where CRISPR-Cas was switched off, where TA plasmid RP4
266 won the competition (competitive ratio = -0.94 ± 0.066; p = 0.00014).

267 While we identified RP4's *parABCDE* TA system as interfering with CRISPR-Cas
268 efficacy in these experiments, we acknowledged that other traits of RP4 may be
269 responsible for the observed effects; RP4 is a 60kB conjugative plasmid carrying many
270 gene cassettes, including additional TA systems. To determine whether our observed
271 effects are caused directly by the *parABCDE* TA system we therefore verified our
272 conclusions by cloning the *par* operon onto a series of cloning vectors with different
273 backbones of varying incompatibility group and offensively competing pKJK5 against
274 these (Figure S4, Supplementary Results 2). This confirmed that CRISPR-Cas on its
275 own can benefit pKJK5, but if a competitor plasmid carries the *par* TA system,
276 CRISPR-Cas is detrimental to pKJK5 in offense – regardless of competitor plasmid
277 backbone.

278 Together, our experiments show that a defensive CRISPR-Cas system was always
279 beneficial to its host plasmid, in agreement with the mathematical model which
280 predicted that a stronger CRISPR-Cas response in defence would benefit the plasmid
281 carrying it regardless of competitor TA status. In addition, we experimentally showed

282 that during a mixed mode of CRISPR-Cas action when invading and competing in
283 naïve hosts, turning on CRISPR-Cas also benefitted the CRISPR-Cas plasmid pKJK5,
284 even in the presence of TA. While this effect was not strong enough to lead to pKJK5
285 winning the competition, there was never a detriment of carrying CRISPR-Cas.

286 In conclusion, we found that the benefit of an offensive CRISPR-Cas system to its host
287 plasmid depends on payload genes encoded on competitor plasmids; namely, a TA
288 system on a competitor means that offensive CRISPR-Cas is detrimental to its
289 plasmid. These limitations were not observed for defensive CRISPR-Cas systems, or
290 CRISPR-Cas plasmids co-invading naïve hosts.

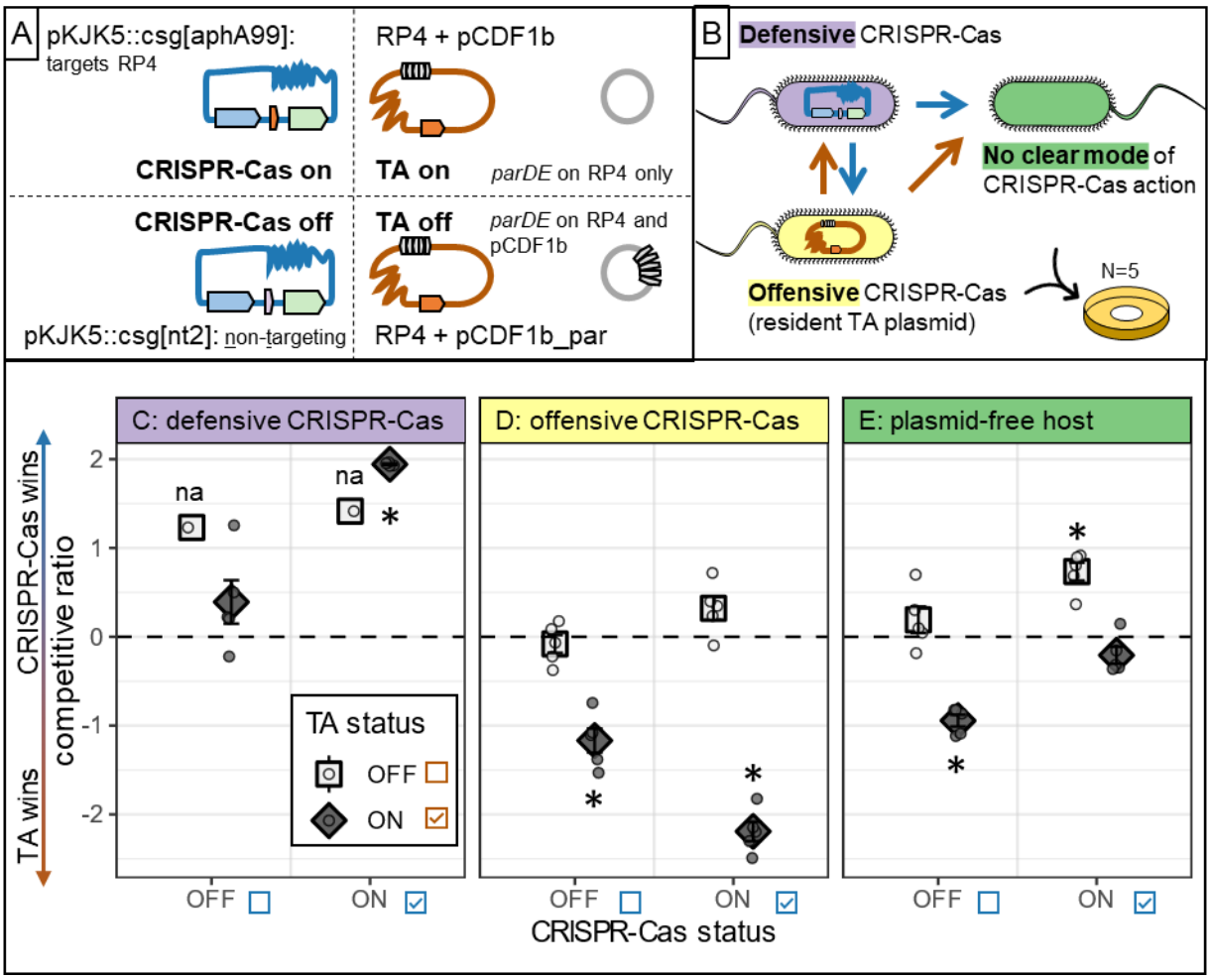

291

292 Figure 2: CRISPR-Cas is beneficial in defence but limited by TA in offense in
293 experimental plasmid competition.

294 A – CRISPR-Cas and TA activity were tweaked on competitor plasmids in a binary
295 manner by switching each system on or off. pKJK5::csg carries a gene cassette
296 encompassing *cas9, sgRNA, GFP* with either RP4-targeting or non-targeting guides,
297 RP4 naturally carries TA system *parABCDE*. B – Plasmids were competed using three
298 *E. coli* DH5α hosts with different plasmid content, allowing us to assess competitive
299 outcome under defensive, offensive, or no clear mode of CRISPR-Cas action. After
300 filter mating, plasmid content of each host was assessed by selective plating.

301 C-E Mean ± standard error of the competitive ratio (log10 of pKJK5-carrying hosts /
302 RP4-carrying hosts) describes outcome of plasmid competition (N=5). Values >0
303 indicate CRISPR-Cas plasmid pKJK5 winning the competition, and values <0 indicate
304 TA plasmid RP4 winning the competition for a certain host. The dashed line indicates
305 a neutral outcome with competitive ratio = 0. Data are presented for treatments in
306 which CRISPR-Cas and TA activity were toggled on or off in all combinations.

307 Stars indicate significant differences from 0 as assessed by T test and Bonferroni
308 adjustment for multiple testing; *$p < 0.005$ with $\alpha = 0.005$; see Table 2 for all p values.
309 na – not assessed due to N=1 after removal of missing values (no carriage of TA
310 plasmid RP4 recorded in 4 out of 5 replicates).

311

312 Plasmid-borne CRISPR-Cas systems preferentially target plasmids lacking TA
313 systems.

314 Our model and experiments suggest that plasmid-borne CRISPR-Cas systems are
315 highly competitive when acting defensively. In contrast, their offensive benefits are
316 limited to conflicts where the competitor plasmid does not encode a TA system. To test
317 whether this constraint is reflected in natural systems, we analysed genomic data to

318 assess the association between CRISPR-Cas targeting and TA presence. If the fitness
319 benefit of CRISPR-Cas systems in plasmid competition is limited by TA systems, we
320 hypothesised that naturally occurring plasmid-borne CRISPR-Cas systems would
321 preferentially target plasmids without TA systems.

322 To answer this question, we analysed existing data on the plasmid-targeting spacers
323 of plasmid-borne CRISPR-Cas systems (Pinilla-Redondo *et al.*, 2022), focusing on
324 identifying which of these targeted plasmids encoded TA systems. The resulting
325 targeting network provided a comprehensive picture of plasmids that were targeted by
326 plasmid-borne CRISPR-Cas systems (N=1340), and the TA systems these targeted
327 plasmids encoded (Figure 3A). In particular, Type II TA were most commonly identified,
328 with *parDE* being detected ~565 times.

329 Within this network, 34% of plasmid-borne CRISPR-Cas systems were Type IV
330 systems (Figure S5A), which function by repressing target gene expression, rather
331 than causing nucleolytic cleavage (Benz *et al.*, 2024; Čepaitė *et al.*, 2024). This mode
332 of action may allow targeted plasmids to persist without triggering post-segregational
333 killing (PSK), potentially obscuring the relationship between targeting and TA
334 presence. Indeed, Type IV-A3-targeted plasmids have been shown to persist when
335 targeted in non-essential regions (Benz *et al.*, 2024). Therefore, we repeated the
336 analysis while excluding Type IV systems. This reduced the number of targeted
337 plasmids to 463, of which only 11% (N=51) encoded TA systems, and none encoded
338 *parDE* (Figure S5B).

339 Correlational analyses on the partitioned data (all CRISPR-Cas types, Type IV only,
340 and non-Type IV) yielded contrasting results. In all cases, Pearson's χ^2 tests confirmed
341 a significant relationship between CRISPR-Cas targeting and TA presence (χ^2 = 94.08,

342 334.48, and 171.83 respectively; $p < 2.2x10^{-16}$), with small effect sizes (φ = 0.073,
343 0.137, and 0.098 respectively). When considering all plasmid-borne CRISPR-Cas
344 types or Type IV only, TA-encoding plasmids were targeted more often than expected
345 under the null hypothesis of no relationship between CRISPR-Cas targeting and TA
346 carriage (residuals = 7.21 and 13.82; $p = 5.71x10^{-13}$ and $1.04x10^{-43}$ respectively;
347 Figure 3B). This contradicts our hypothesis that plasmid-borne CRISPR-Cas systems
348 should preferentially target plasmids lacking TA systems.

349 In contrast, when we excluded Type IV CRISPR-Cas systems, the association
350 between CRISPR-Cas targeting and TA carriage reversed: fewer TA-encoding
351 plasmids were targeted than expected (residual = -10; $p = 1.49x10^{-23}$), consistent with
352 our experimental data and model predictions.

353 Overall, these results indicate that nucleolytic plasmid-borne CRISPR-Cas systems
354 preferentially target plasmids lacking TA systems. This supports and extends our
355 model and experimental findings to natural systems across diverse CRISPR-Cas and
356 TA system types. We conclude that nucleolytic, plasmid-borne CRISPR-Cas systems
357 provide significant defensive benefits, even in the face of TA. In contrast, their benefits
358 in offence are constrained by the presence of TA systems on competitor plasmids.

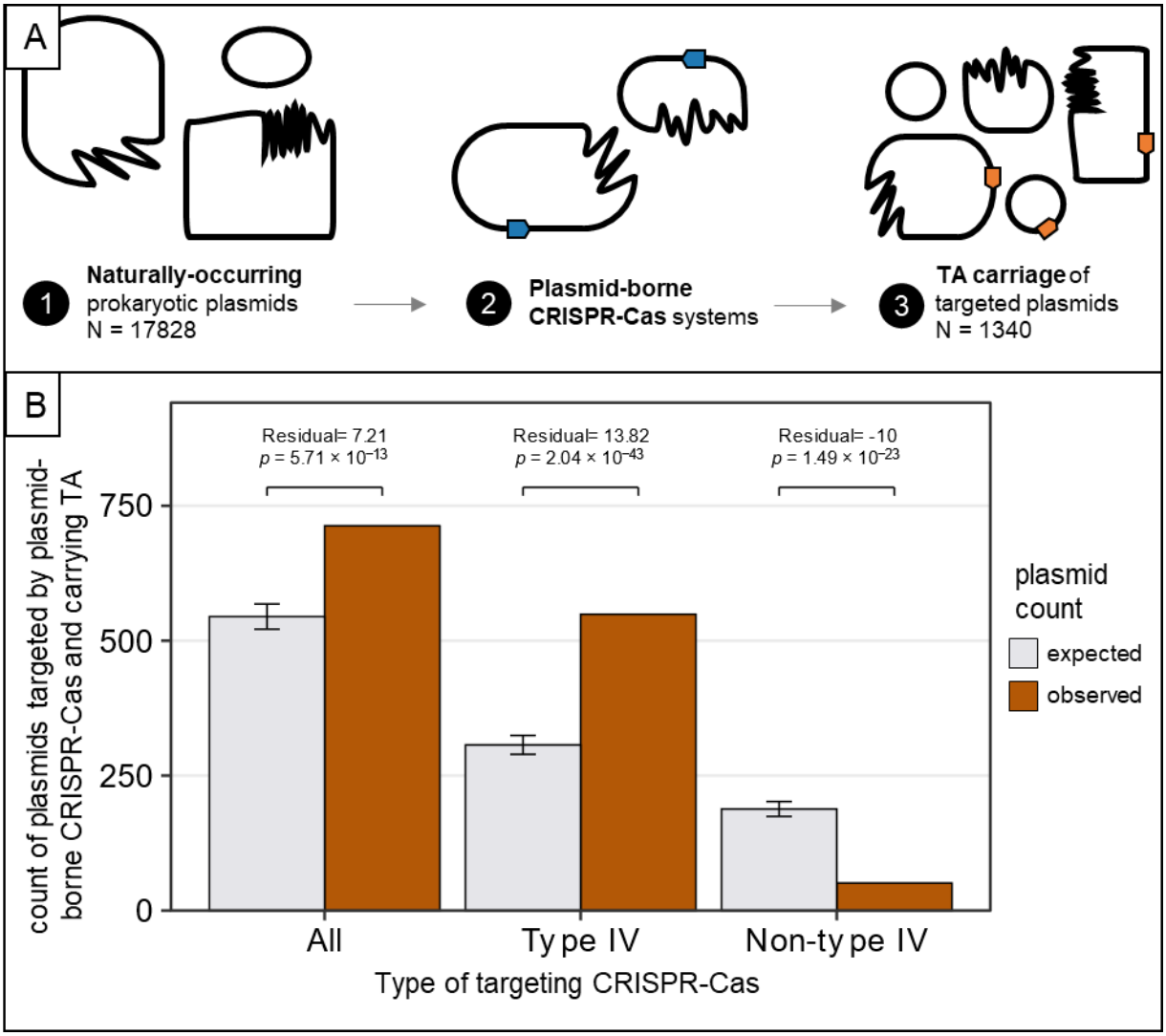

Figure 3: Plasmid-borne CRISPR-Cas systems (excluding Type IV) avoid targeting plasmids with toxin-antitoxin systems.

A – Naturally-occurring plasmid-borne CRISPR-Cas systems and the plasmids they target (Pinilla-Redondo *et al.*, 2022) were analysed for toxin-antitoxin (TA) carriage.

B - Comparison of observed vs. expected counts of targeted plasmids encoding TA by CRISPR-Cas type. Brown bars show the observed counts of plasmids in each group compared to the expected counts (grey bars) under the null hypothesis of independence between targeting and TA presence. Error bars represent standard error. Residuals and *p* values are presented after a Pearson's χ^2 test. Full contingency

369 tables for all categories of plasmids can be found in Figure S6 (targeted or not targeted
370 by CRISPR-Cas, coding or not coding for TA).

371

372 **Discussion**

373 In this work, we uncovered the limitations of CRISPR-Cas in plasmid competition.
374 Mathematical modelling predicted that when plasmids compete within co-infected
375 cells, CRISPR-Cas can provide a benefit to the plasmid it resides on. However, when
376 the competitor plasmid encodes a strong toxin-antitoxin (TA) system, CRISPR-Cas is
377 only beneficial when defensive and resident in a host. We further observed this
378 outcome of CRISPR-Cas- and TA-plasmid competition in an experimental model
379 system, showing how offensive CRISPR-Cas becomes a liability when targeting a
380 resident TA plasmid, while defensive and co-invading CRISPR-Cas could provide a
381 benefit even when competing against a TA plasmid. Finally, we further tested our
382 theory and generalised our experimental findings by bioinformatically showing that
383 plasmid-borne nucleolytic CRISPR-Cas systems avoid targeting other plasmids
384 carrying TA systems.

385 A crucial role of TA in plasmid establishment, spread, and maintenance has previously
386 been documented (Cooper and Heinemann, 2000; Cooper *et al.*, 2010; Rankin *et al.*,
387 2012). Our data adds to this broad utility of TA throughout a plasmid's life cycle, as we
388 found that TA contributed to TA plasmid competitiveness in nearly all experimental
389 scenarios (Figure 2). Underlining this, our mathematical model predicted that unlike
390 CRISPR-Cas (the benefit of which diminished when competing TA was stronger), TA
391 became more beneficial in the presence of a stronger CRISPR-Cas response on the
392 competitor plasmid when the TA plasmid was resident (Figure S2B).

393 Regardless, TA and CRISPR-Cas show striking similarity in that they benefit their own
394 plasmid more when acting defensively than offensively (Figure 2, Figure S2). It is well
395 established that plasmids are more fit when residing in a host cell than when
396 conjugating into a new host (reviewed in (San Millan and MacLean, 2017)):
397 conjugation itself is costly (e.g. by SOS-response activation; (Baharoglu *et al.*, 2010)),
398 a novel plasmid is associated with a high transient fitness cost (Prensky *et al.*, 2021),
399 and existing plasmid-host pairs can benefit from compensatory mutations to
400 ameliorate fitness costs (Hall *et al.*, 2019). Here, we add to this body of evidence by
401 showing that specific plasmid-encoded genes, namely CRISPR-Cas and TA, also
402 provide a higher benefit to vertically transferred plasmids than to those that are
403 horizontally transferred when facing plasmid competition. These findings can help
404 explain naturally observed repression of conjugative machinery (Lundquist and Levin,
405 1986).

406 Recent modelling showed that plasmid cost is a key determinant of whether a plasmid
407 carrying TA can become established in a bacterial population carrying (chromosomally
408 encoded) CRISPR-Cas systems (Siedentop *et al.*, 2024). In support of this, modelling
409 showed that plasmids struggle to become established during plasmid competition
410 when co-infection comes with a significant cost (Igler *et al.*, 2021). We do not directly
411 measure plasmid costs in our experimental system, but our mathematical model
412 conceptualises the presence of both CRISPR-Cas and TA as a costly state due to a
413 PSK effect. Experimentally, we are likely overinflating the strength of TA compared to
414 natural populations: we carried out the experimental work in DH5α, a recA- *E. coli*
415 strain. RecA is implicated in *parDE* TA function, where recA- strains typically see
416 survival rates ~3 orders of magnitude lower than recA+ strains (Fraikin and
417 Van Melderen, 2024). Nevertheless, our bioinformatic analyses confirms that our

418 experimental results are generalisable by revealing a dissociation between plasmid-
419 borne CRISPR-Cas targeting and competitor plasmid TA carriage.

420 Our findings clearly show that due to their offensive capability, plasmid-borne CRISPR-
421 Cas systems are under different selective pressures than chromosomally encoded
422 CRISPR-Cas systems. This helps explain the distribution and mobility of microbial
423 defence systems, where certain systems are more commonly found on specific mobile
424 genetic elements (MGEs) rather than the bacterial chromosome (for instance, a
425 number of defences are commonly found on prophage; reviewed in (Georjon and
426 Bernheim, 2023; Patel and Maxwell, 2023). Similarly, our results indicate that it is
427 unsurprising that certain types of CRISPR-Cas lacking a nuclease, such as Type IV,
428 are preferentially found on plasmids (Pinilla-Redondo *et al.*, 2022). In our
429 bioinformatics analysis, we found that only nucleolytic, non-Type IV, plasmid borne
430 CRISPR-Cas systems avoid targeting plasmids carrying TA systems. Based on this,
431 we hypothesise that plasmid-borne CRISPR-Cas systems adopt different evolutionary
432 strategies in light of competitor plasmids encoding TA. A plasmid-borne CRISPR-Cas
433 system can avoid targeting TA plasmids to overcome limitations caused by TA in
434 offense, as showcased in our data and bioinformatics analysis. An alternative
435 evolutionary scenario can involve the loss of nucleolytic activities, as seen for plasmid-
436 borne Type IV and Type V-M (Wu *et al.*, 2022) CRISPR-Cas systems, which would not
437 have these limitations and can target TA-carrying plasmids without paying the costs of
438 PSK induction. In addition to silencing rather than cleaving DNA, Type IV CRISPR-
439 Cas systems may overcome TA activity by additional means. For instance, the
440 propensity of Type IV CRISPR-Cas systems to co-opt their host's spacer acquisition
441 machinery (Newire *et al.*, 2020; Benz *et al.*, 2024) may strengthen Type IV CRISPR-
442 Cas's role in defence (while resident in its host, the CRISPR-Cas system can acquire

443 new spacers to defend from MGEs), while dampening its role in offense (when moving
444 to a new host, the CRISPR-Cas system cannot acquire new spacers until established).
445 A dampened CRISPR-Cas strength in offense may allow CRISPR-Cas mobility by
446 circumventing autoimmunity arising from chromosomal targeting. The proposed
447 evolutionary history of Type IV CRISPR-Cas systems supports the hypothesis that
448 plasmid-borne CRISPR-Cas systems adopt different evolutionary strategies to remain
449 effective in light of TA: nucleolytic Type III CRISPR-Cas lost its HD nuclease domain
450 and diverged towards gene silencing activity by association with helicase DinG over
451 evolutionary timescales (Moya-Beltrán *et al.*, 2021). Overall, the association between
452 TA and the effectivity of CRISPR-Cas in plasmid competition helps explain the
453 distribution and mobility of bacterial defence systems and the propensity of certain
454 defences to associate with particular MGEs.

455 Throughout this work, we assayed plasmid competition outcome within individual
456 plasmid hosts. Despite this limitation, our work has further-reaching implications. On
457 a population level, within-host plasmid competition may be particularly relevant to
458 highly permissive plasmid hosts – bacteria in which the cost of plasmid maintenance
459 is low and which can cause persistence of plasmids on a community level (Li *et al.*,
460 2018; Alonso-del Valle *et al.*, 2021), or in hosts closely associated with certain plasmid
461 lineages, such as clinically problematic bacterial strains of *E. coli* Sequence Type (ST)
462 131 and their IncF plasmids (Kondratyeva *et al.*, 2020). Our results could inform
463 predictions of community-level plasmid persistence, where a resident CRISPR-Cas
464 plasmid in such highly permissive plasmid hosts may prevent their colonisation by TA-
465 encoding competitor plasmids, and thus prevent TA plasmid dissemination throughout
466 the microbial community. In addition to making predictions about plasmid prevalence,
467 our work can inform the use of CRISPR-Cas delivery tools (engineered plasmids used

468 to directly kill or resensitise bacteria to antibiotics through removal of AMR-encoding
469 plasmids (Pursey *et al.*, 2018; Sünderhauf *et al.*, 2023b)). Our work indicates that
470 CRISPR-Cas delivery tools will be more effective when delivered prophylactically, i.e.
471 when CRISPR-Cas is allowed to act defensively rather than offensively. When they
472 are required to act offensively, other factors such as target plasmid copy number and
473 compatibility can inform optimal CRISPR-Cas delivery tool design (Kippnich *et al.*,
474 2024). Alternatively, designing offensive CRISPR-Cas tools to intentionally target TA-
475 encoding multidrug-resistance plasmids could be a means of destabilizing pathogenic
476 bacteria rather than just eliminating their problematic plasmids.

477

478 In this work, we describe how the relevance of CRISPR-Cas to plasmid competition
479 depends on its mode of action: defensive CRISPR-Cas is universally beneficial, but
480 the benefit of offensive CRISPR-Cas can be limited by TA genes present on competitor
481 plasmids. This work underlines the utility of TA systems to plasmid competition and
482 explains their ubiquity, and in addition may help to predict which plasmids can become
483 established in clinically relevant species and communities. Further, we help explain
484 the distribution of bacterial defence systems by uncovering under which conditions
485 plasmid-borne CRISPR-Cas systems are selected for, and inform the use of CRISPR-
486 Cas based technologies.

487

488 **Methods**

489 <u>Mathematical model</u>

490 Mathematical modelling was carried out using Wolfram Mathematica v14.1. Equations
491 E9-E10 (see Supplementary Results 1) were imported into R version 4.3.2. Output

492 plots were generated using RStudio version 2023.09.1+494 with the following
493 packages: dplyr, ggplot2.

494

495 Plasmids and strains

496 Plasmids and strains used in this study are summarised in Table 1. *Escherichia coli*
497 DH5α strains DH5α::CmR, DH5α::GmR, and DH5α::SmR were constructed by
498 electroporating DH5α with pBAM1-Gm, pBAM1-Sm, and pBAM1-Cm respectively and
499 selecting for resistant recombinants; resistance gene insertion was confirmed by PCR
500 (Martínez-García *et al.*, 2011; Dimitriu *et al.*, 2022) and verifying their respective
501 resistant phenotypes after transfer in the absence of antibiotics.

502 RP4-targeting pKJK5::csg[aphA99] ('CRISPR-Cas on' version of pKJK5) was
503 constructed using λ-red mediated recombineering and pKJK5 as a template, as
504 described in (Sünderhauf *et al.*, 2023b) with the exception that *cas9*, *sgRNA*
505 (programmed to target *aphA* with specificity AAATGGGCGCGTGATAAGGT) and *gfp*
506 were inserted into pKJK5's *intI1* gene. Non-targeting control pKJK5::csg[nt2]
507 ('CRISPR-Cas off' version of pKJK5) was previously published as pKJK5::gfp^{PL}
508 (Sünderhauf *et al.*, 2023a) and carries a random non-functional *sgRNA*.

509 Vector pOGG99_par was constructed by deleting genes from pOPS0378 (Mendoza-
510 Suárez *et al.*, 2020) to generate a minimal vector: *mCherry* was removed by digestion
511 with EcoRI, extraction, and re-ligation of the 6043 bp band. Next, site-directed
512 mutagenesis of *aphA* was carried out using primers pOGG0_mut_fw and
513 pOGG0_mut_rv and Thermo Scientific's site-directed mutagenesis kit according to
514 manufacturer's instructions. In this way, the nucleotide at position 96 within *aphA* was
515 silently mutated from C to G to bring the gene sequence in line with that found on our

516 laboratory's version of RP4 and allow targeting by pKJK5::csg[aphA99]. Successful
517 mutation was confirmed by Sanger sequencing of the finished plasmid using primer
518 pOGG0_sequence. pOGG99 was constructed by excising *parABCDE* from
519 pOGG99_par: pOGG99_par was digested with BlpI and BglII, the 3664 bp fragment
520 was extracted and religated with annealed and phosphorylated linker oligos
521 (pOGG99_parRemoval_top & btm). This yielded pOGG99, a version of pOGG99_par
522 where *parABCDE* are replaced with a multiple cloning site module.

523 Vector pHERD99 was constructed by annealing oligos aphA99PAM_top and
524 aphA99_btm and inserting them into pHERD30T's HindIII and KpnI restriction sites
525 following standard molecular cloning protocols. Vector pSEVA251-99 was constructed
526 by site-directed mutagenesis of pSEVA251's *aphA* gene as described for
527 pOGG99_par above.

528 Vectors pCDF1b_par, pHERD99_par, and pSEVA251-99_par were constructed by
529 *parABCDE* amplification using pOGG99_par as a template and primers par_fw and
530 par_rv with high-fidelity Phusion polymerase (NEB) and insertion into pCDF1b,
531 pHERD99's, and pSEVA251-99's KpnI restriction site respectively. This *parABCDE*
532 operon is 99.96% identical to RP4's with a single nucleotide mismatch in the non-
533 coding area between *parA* and *parB*.

534 All cloned plasmids were subjected to long-read sequencing by Plasmidsaurus using
535 Oxford Nanopore Technology with custom analysis and annotation. Annotated
536 sequences are deposited on Genbank with IDs listed in Table 1.

537

538

539

540 **Table 1: Strains, Plasmids, and primers**

Strains			
Name	**Shorthand**	**Notes**	**Reference**
Escherichia coli DH5α	DH5α		Common laboratory strain
Escherichia coli K12::mCherry	K12::mCherry	Chromosomal Km^R, mCherry, lacI insertion	(Klümper *et al.*, 2015)
Escherichia coli DH5α::CmR	DH5α::CmR	Chromosomal *cat* insertion	*This study*
Escherichia coli DH5α::GmR	DH5α::GmR	Chromosomal *aacC1* insertion	*This study*
Escherichia coli DH5α::SmR	DH5α::SmR	Chromosomal *aad* insertion	*This study*
Plasmids			
Plasmid	**Resistance and Payload**	**Notes**	**Reference**
pKJK5::csg[aphA99]	Tetracycline, Trimethoprim, CRISPR-Cas9 cassette targeted towards *aphA*	"CRISPR-Cas on" version of pKJK5::csg	*This study*
pKJK5::csg[nt2]	Tetracycline, Trimethoprim, non-targeting CRISPR-Cas9 cassette	"CRISPR-Cas off" version of pKJK5::csg. Previously referred to as pKJK5::gfp^{PL}	(Sünderhauf *et al.*, 2023a)
pHERD30T	Gentamicin	pBR322 vector	(Qiu *et al.*, 2008)
pHERD99	Gentamicin, includes [aphA99] target site	Genbank acc. OR900359	*This study*
pHERD99_par	Gentamicin, [aphA99] target site, *parABCDE*	Genbank acc. OR900360	*This study*
pCDF1b	Streptomycin		Novagen (EMD Millipore)
pCDF1b_par	Streptomycin, *parABCDE*	Genbank acc. OR900361	*This study*
pSEVA251	Kanamycin	IncQ vector; Genbank acc. JX560330	(Silva-Rocha *et al.*, 2013)
pSEVA251-99	Kanamycin (targetable by pKJK5::csg[aphA99])	Genbank acc. PV231316	*This study*
pSEVA251-99_par	Kanamycin, *parABCDE*	Genbank acc. PV231317	*This study*

pOPS0378	Kanamycin, mCherry, *parABCDE*	Addgene #133229	(Mendoza-Suárez *et al.*, 2020)
pOGG99	Kanamycin	IncP vector; Genbank acc. PV231318	*This study*
pOGG99_par	Kanamycin, *parABCDE*	Genbank acc. PV231319	*This study*
RP4	Tetracycline, Kanamycin, Ampicillin, *parABCDE*	Genbank acc. L27758	(Pansegrau *et al.*, 1994)
pBAM1-Gm	Ampicillin, Gentamicin	Tn5 *aacC1* transposon	(Martínez-García *et al.*, 2011)
pBAM1-Sm	Ampicillin, Streptomycin	Tn5 *aad* tranposon	(Martínez-García *et al.*, 2011)
pBAM1-Cm	Ampicillin, Chloramphenicol	Tn5 *cat* transposon	(Dimitriu *et al.*, 2022)

Primers and sequences

Name	**Sequence (5' → 3')**
[aphA99]	AAATGGGCGCGTGATAAGGT
[nt2]	GTTTTCTGCCTGTCGATCCAGTTTTAGAGCTCTAAAACTGGATCGACAGGCAGAAAACATGTCGATCCA
par_fw	TCGGTACCTGCATGAGCTTGTGGAAGTG
par_rv	CAGGTACCTGCTCAACAGGTTCGCA
aphA99PAM_top	AGCTTAAATGGGCGCGTGATAAGGTTGGTAC
aphA99PAM_btm	CAACCTTATCACGCGCCCATTTA
pOGG0_mut_fw	TGGGCGCGTGATAAGGTGGGTCAGAGCGGC
pOGG0_mut_rv	TTTATAGCCATACAGATCCGCATCCATGTTGCTGTTCAGACGC
pOGG0_sequence	TATTGGTGAGAATCCAGGCA
pOGG99_parRemoval_top	TGAGCCAAGCTTGCATGCCTGCAGGTCGACTCTAGAGGATCCCCGGGTACCGAGCTCGAATTCACTA
pOGG99_parRemoval_btm	GATCTAGTGAATTCGAGCTCGGTACCCGGGGATCCTCTAGAGTCGACCTGCAGGCATGCAAGCTTGGC

Culture conditions

Unless otherwise stated, all strains were cultured shaking 180 rpm in LB broth or statically on LB plates at 37˚C. Where appropriate, cultures or plates were supplemented with the following antibiotics at the following concentrations: Ap – 100 µg/mL ampicillin; Cm – 25µg/mL chloramphenicol; Gm – 50 µg/mL gentamicin; Km –

547 50 µg/mL kanamycin; Sm – 50 µg/mL streptomycin; Tc – 12 µg/mL tetracycline; Tmp
548 – 10 µg/mL trimethoprim.

549

550 Conjugation experiments

551 In three-strain competitions (Figure 2), bacterial hosts used were *E. coli* DH5α::SmR
552 containing pKJK5::csg, *E. coli* DH5α::CmR containing RP4, and *E. coli* DH5α::GmR.
553 All three strains either also contained empty vector pCDF1b, or pCDF1b_par for TA-
554 off treatments.

555 In two-strain competitions (Figure S4), *E. coli* K12::mCherry containing pKJK5::csg
556 was used as donor, and the recipient was *E. coli* DH5α::CmR containing either RP4,
557 pHERD99, pSEVA251-99, pOGG99, or their *par*-encoding derivatives.

558 To turn CRISPR-Cas activity on or off, we used two different pKJK5::csg variants with
559 fixed targeting specificity: pKJK5::csg[aphA99] was programmed to target RP4's *aphA*
560 gene, and pKJK5::csg[nt2] encoded a non-functional sgRNA with a random 69-nt
561 target sequence that is not present in the model system (plasmid pKJK5::gfp^{PL};
562 (Sünderhauf *et al.*, 2023a)).

563 Single colonies from streak plates of mating partners were suspended in 15-25 mL LB
564 with antibiotics appropriate to maintain their plasmid content (see Table 1) and grown
565 overnight. These T0 cultures were then washed twice with 0.9% (w/v) NaCl and
566 adjusted to OD600 = 0.5. Washed, OD-adjusted cultures were filter mated in a 1:1(:1)
567 ratio:

568 Filter matings were carried out using a 12-stream Millipore vacuum pump, sterilised
569 with 70% Ethanol and UV light before and after each batch of filter mating and

570 assembled in a Cat2 biosafety cabinet. For each mating, a 0.22 µm glass microfibre
571 filter (Whatman) was placed onto a vacuum pump position, dampened with 200 µL
572 sterile 0.9% NaCl, and topped with a 0.22 µm cyclopore membrane (Whatman). Fully
573 assembled filter positions were equilibrated by applying a vacuum until 2 mL of 0.9%
574 NaCl were pumped through. Next, 1 mL of OD-adjusted donors and 1 mL of OD-
575 adjusted recipients (or 600 µL of each mating partner in 3-strain competitions) were
576 added to each filter position together with 1 mL 0.9% NaCl, and a vacuum applied until
577 the strain mix was pumped through (N=5). Control matings always included donor-
578 only, recipient-only (and naïve-strain-only where appropriate), and buffer-only sterility
579 controls and yielded results as expected. Cyclopore membranes were placed cell-
580 side-up onto a 10% LB plate (supplemented with 0.9% NaCl) and incubated at 37˚C
581 for 36 hours. Then, cells were recovered by placing each filter into 3 mL of 0.9% NaCl
582 and vortexed for 15 seconds. This cell suspension was frozen in 20% (w/v) glycerol at
583 -70˚C and plated onto selective plates with various antibiotic regimes to assess strain
584 prevalence and strains' plasmid content.

585 Selective plating

586 Samples were plated in 5 µL droplets in dilutions ranging from 10^0-10^{-7} onto LB
587 medium containing different combinations of antibiotics. Cm, and Gm were used to
588 select for DH5α::Cm and DH5α::Gm respectively, and combining these antibiotics with
589 Tmp and Km allowed growth of only DH5α hosts carrying pKJK5 and RP4 respectively.
590 Colonies were counted at the most appropriate dilution, and GFP fluorescence of
591 pKJK5::csg-containing colonies confirmed stringency of selective regimes.

592 To assess overall sample composition and plasmid content of the DH5α::SmR host,
593 we plated 50 µL of a 10^{-5} dilution of each replicate onto LB plates without selection

594 and suspended 96 colonies of each sample in 250 µL LB each following overnight
595 incubation. Previous assessment of colonies from selective plates sub-cultured on
596 non-selective media indicated that RP4 and pKJK5::csg did not become lost over this
597 timeframe in the absence of selection. The 96 clones picked from each replicate were
598 then replica-stamped onto plates containing no selection, Cm, Gm, Km, and/or, Tmp.
599 Clones growing on LB, but not LB supplemented with Cm or with Gm were scored as
600 DH5α::SmR clones, and the Km / Tmp selective plates were used to score their
601 plasmid content.

602 Plasmid competitive ratio

603 We calculated pKJK5 and RP4's competitive ratio as follows:

604 $$competitive\ ratio = \log\left(\frac{\text{hosts containing pKJK5}}{\text{hosts containing RP4}}\right)$$

605 This gives a measure of which plasmid is more frequent in a certain host and therefore
606 won the competition for the host at the end of the experiment. Positive competitive
607 ratios indicate pKJK5 winning the competition, negative ratios indicate RP4 winning,
608 and ratios ≈ 0 indicate equal carriage of pKJK5 and RP4 in the host.

609

610 Statistical analyses

611 Colony counts on all selective plates from all experiments, together with plasmid
612 competitive ratios used to produce figures are available in supplementary material.

613 Data processing, data visualisation, and statistical analyses were carried out using R
614 version 4.3.2 and RStudio version 2023.09.1+494 with the following packages:
615 flextable, dplyr, readr, tidyr, ggplot2.

616 *Competitive ratio*

617 We carried out one-sample T tests and Bonferroni adjustment for multiple testing to
618 test for significant differences of plasmid competitive ratio to 0, indicating either RP4
619 or pKJK5 winning the plasmid competition. Statistical significance of 'TA off'
620 competitive ratio in DH5α::SmR could not be assessed due to N=1, as no RP4 carriage
621 was recorded in most replicates. For all *p* values, see Table 2. Competitive ratios of
622 vector competitions (Figure S4) were assessed in the same way. For all *p* values, see
623 Table 3.

624 Table 2: T tests adjusted for multiple testing (Figure 2). Significant values after
625 Bonferroni adjustment in bold. Host refers to *E. coli* DH5α chromosomal tag
626 identity; S – SmR (defensive CRISPR-Cas), C – CmR (offensive CRISPR-Cas),
627 G – GmR (naïve host).

CRISPR-Cas status	host	TA status	p value (unadjusted)
on	C	on	**0.0000365582932**
on	C	off	0.0719892969523
on	G	on	0.0966797444140
on	G	off	**0.0018640114602**
on	S	on	**0.0000002614983**
off	C	on	**0.0009984435471**
off	C	off	0.4685379085725
off	G	on	**0.0001373821288**
off	G	off	0.2664700148622
off	S	on	0.1845008343480

Bonferroni-adjusted significance threshold α = 0.005

628 Table 3: T tests adjusted for multiple testing (Figure S4). Significant values after
629 Bonferroni adjustment in bold.

630

plasmid_backbone	CRISPR_status	par_status	p value (unadjusted)
RP4	off	on	**0.00241983623**
RP4	on	on	**0.00129308853**
pHERD99	off	off	**0.00196693917**
pHERD99	off	on	**0.00281440466**
pHERD99	on	off	**0.00075665162**
pHERD99	on	on	**0.00096428453**
pOGG99	off	off	0.00472375166
pOGG99	on	off	0.01437141407
pSEVA251-99	off	off	**0.00198288741**
pSEVA251-99	off	on	**0.00102338623**
pSEVA251-99	on	off	**0.00055796800**
pSEVA251-99	on	on	**0.00001333917**

Bonferroni-adjusted significance threshold α = 0.0042

631

632 Additionally, we fitted separate Generalised Linear Models to data generated in two-
633 strain competitions (Figure S4). GLMs were chosen so inclusion of additional variables
634 (e.g. replicate and position on filter pump) could be tested, and the final models chosen
635 for not including non-significant explanatory variables and upholding model
636 assumptions. For model structures and coefficients see Table 4. pHERD99 and
637 pSEVA251-99 data were followed up by Tukey's HSD test, see Table 5. Note that
638 statistical models were constructed based on inverted data (-(competitive ratio)).

639

Table 4: GLM structures and coefficients for Figure S4.

RP4 model comprat ~ CRISPR_status

	Estimate	Standard Error	z value	Pr(>|z|)	
(Intercept)	0.487	0.110	4.417	0.0022	**
CRISPR_statuson	0.629	0.156	4.032	0.0038	**

*Signif. codes: 0 <= '***' < 0.001 < '**' < 0.01 < '*' < 0.05*

(Dispersion parameter for gaussian family taken to be 0.06080916)
Null deviance: 1.475 on 9 degrees of freedom
Residual deviance: 0.4865 on 8 degrees of freedom

pOGG99 model comprat ~ CRISPR_status

	Estimate	Standard Error	z value	Pr(>|z|)	
(Intercept)	5.503	0.273	20.184	0.0000	***
CRISPR_statuson	-4.707	0.323	-14.590	0.0000	***

*Signif. codes: 0 <= '***' < 0.001 < '**' < 0.01 < '*' < 0.05*

(Dispersion parameter for gaussian family taken to be 0.1486764)
Residual deviance: 0.7434 on 5 degrees of freedom

pHERD99 model comprat ~ CRISPR_status*TA_status

	Estimate	Standard Error	z value	Pr(>|z|)	
(Intercept)	0.871	0.156	5.573	0.0000	***
CRISPR_statuson	-2.113	0.221	-9.563	0.0000	***
TA_statuson	0.356	0.221	1.609	0.1271	
CRISPR_statuson:TA_statuson	2.391	0.312	7.652	0.0000	***

*Signif. codes: 0 <= '***' < 0.001 < '**' < 0.01 < '*' < 0.05*

(Dispersion parameter for gaussian family taken to be 0.1220155)
Null deviance: 25.33 on 19 degrees of freedom
Residual deviance: 1.952 on 16 degrees of freedom

pSEVA251-99 model comprat ~ CRISPR_status*TA_status

	Estimate	Standard Error	z value	Pr(>|z|)	
(Intercept)	1.004	0.117	8.565	0.0000	***
CRISPR_statuson	-0.509	0.166	-3.072	0.0073	**
TA_statuson	-0.158	0.166	-0.955	0.3539	
CRISPR_statuson:TA_statuson	3.603	0.234	15.370	0.0000	***

*Signif. codes: 0 <= '***' < 0.001 < '**' < 0.01 < '*' < 0.05*

(Dispersion parameter for gaussian family taken to be 0.06870578)
Null deviance: 39.18 on 19 degrees of freedom
Residual deviance: 1.099 on 16 degrees of freedom

Table 5: Tukey's HSD results for Figure S4CD.

pHERD99 (CRISPR:TA status)	diff	lwr	upr	p value (adjusted)
off:off-on:off	2.1126735	1.480613329	2.7447337	**2.83E-07**
off:on-on:off	2.4682169	1.836156677	3.1002771	**3.21E-08**
on:on-on:off	2.7462391	2.114178923	3.3782993	**6.92E-09**
off:on-off:off	0.3555433	-0.276516842	0.9876035	4.01E-01
on:on-off:off	0.6335656	0.001505405	1.2656258	**4.94E-02**
on:on-off:on	0.2780222	-0.354037943	0.9100824	6.01E-01
pSEVA251-99 (CRISPR:TA status)	diff	lwr	upr	p value (adjusted)
off:on-on:off	0.3510055	-0.12328835	0.8252993	1.90E-01
off:off-on:off	0.5092798	0.03498597	0.9835737	**3.32E-02**
on:on-on:off	3.4450619	2.97076801	3.9193557	**3.44E-12**
off:off-off:on	0.1582743	-0.31601952	0.6325682	7.76E-01
on:on-off:on	3.0940564	2.61976252	3.5683502	**1.51E-11**
on:on-off:off	2.9357820	2.46148820	3.4100759	**3.27E-11**

Streptomycin resistant c.f.u.

The log10 of proportion of streptomycin resistant c.f.u. presented in Figure S3 followed a normal distribution and was assessed by one-sample T tests and Bonferroni adjustment for multiple testing for differences to 0 (log10 of 1; complete maintenance of bystander vector pCDF1b). No differences were statistically significant (Table 4).

Table 6: T tests adjusted for multiple testing (Figure S3). Significant values after Bonferroni adjustment in bold.

CRISPR status	TA status	p value (unadjusted)
off	off	0.54312707
off	on	0.80081603
on	off	0.04135612
on	on	0.98506756

Bonferroni-adjusted significance threshold α = 0.0125

652 Bioinformatic Analyses

653 The sequences of 17828 de-replicated plasmid found across prokaryotic genomes
654 (Pinilla-Redondo *et al.*, 2022) were retrieved from NCBI using rentrez (Winter, 2017).
655 CRISPR-Cas presence and targeting information were adopted from (Pinilla-Redondo
656 *et al.*, 2022). Plasmid open reading frames were predicted with prodigal v2.6.3 (Hyatt
657 *et al.*, 2010). Toxin-antitoxin nucleotide or protein sequences were retrieved from
658 TADB v3.0 (Guan *et al.*, 2024). To identify complete toxin-antitoxin systems, plasmids
659 were searched with BLAST v2.16.0 (Camacho *et al.*, 2009) and hits were filtered for
660 cases where both a toxin and antitoxin component were directly adjacent. Statistical
661 analyses were run using R v4.4.2 base functions.

662

663 **Acknowledgements**

664 The authors would like to thank Mario Mestre (KU Copenhagen, Denmark) and Edze
665 Westra (University of Exeter, UK) for stimulating and inspiring discussions and
666 enthusiasm.

667 For the purpose of open access, the author has applied a 'Creative Commons
668 Attribution (CC BY) licence to any Author Accepted Manuscript version arising from
669 this submission.

670 **Funding**

671 DS was supported in part by grant MR/N0137941/1 for the GW4 BIOMED MRC DTP,
672 awarded to the Universities of Bath, Bristol, Cardiff and Exeter from the Medical
673 Research Council (MRC)/UKRI. JRR was supported by a summer studentship from
674 the Lister Institute for Preventative Medicine. LJP and RPR were supported by

research grant VIL60763 from VILLUM FONDEN. SPB acknowledges funding from the US National Science Foundation (NSF 2321502). WHG and SvH acknowledge funding from the JPI-AMR HARISSA programme (MISTAR; MR/W031191/1), and in addition SvH acknowledges funding from the Biotechnology and Biological Sciences Research Council (BB/R010781/1; BB/S017674/1) and the Lister Institute for Preventative Medicine.

References

Adamczyk, M. and Jagura-Burdzy, G. 2003. Spread and survival of promiscuous IncP-1 plasmids. *Acta Biochimica Polonica* 50: 425–453.

Alonso-del Valle, A., León-Sampedro, R., Rodríguez-Beltrán, J., DelaFuente, J., Hernández-García, M., Ruiz-Garbajosa, P., Cantón, R., Peña-Miller, R. and San Millán, A. 2021. Variability of plasmid fitness effects contributes to plasmid persistence in bacterial communities. *Nature Communications* 12: 2653.

Baharoglu, Z., Bikard, D. and Mazel, D. 2010. Conjugative DNA Transfer Induces the Bacterial SOS Response and Promotes Antibiotic Resistance Development through Integron Activation. *PLOS Genetics* 6: e1001165.

Bahl, M.I., Hansen, L.H., Goesmann, A. and Sørensen, S.J. 2007. The multiple antibiotic resistance IncP-1 plasmid pKJK5 isolated from a soil environment is phylogenetically divergent from members of the previously established α, β and δ sub-groups. *Plasmid* 58: 31–43.

Beamud, B., Benz, F. and Bikard, D. 2024. Going viral: The role of mobile genetic elements in bacterial immunity. *Cell Host & Microbe* 32: 804–819.

Benz, F., Camara-Wilpert, S., Russel, J., Wandera, K.G., Čepaitė, R., Ares-Arroyo, M., Gomes-Filho, J.V., Englert, F., Kuehn, J.A., Gloor, S., Mestre, M.R., Cuénod, A., Aguilà-Sans, M., Maccario, L., Egli, A., Randau, L., Pausch, P., Rocha, E.P.C., Beisel, C.L., Madsen, J.S., Bikard, D., Hall, A.R., Sørensen, S.J. and Pinilla-Redondo, R. 2024. Type IV-A3 CRISPR-Cas systems drive inter-plasmid conflicts by acquiring spacers in trans. *Cell Host & Microbe* 32: 875-886.e9.

Camacho, C., Coulouris, G., Avagyan, V., Ma, N., Papadopoulos, J., Bealer, K. and Madden, T.L. 2009. BLAST+: architecture and applications. *BMC Bioinformatics* 10: 421.

Čepaitė, R., Klein, N., Mikšys, A., Camara-Wilpert, S., Ragožius, V., Benz, F., Skorupskaitė, A., Becker, H., Žvejytė, G., Steube, N., Hochberg, G.K.A., Randau, L., Pinilla-Redondo, R., Malinauskaitė, L. and Pausch, P. 2024. Structural variation of types IV-A1- and IV-A3-mediated CRISPR interference. *Nature Communications* 15: 9306.

Cooper, T.F. and Heinemann, J.A. 2000. Postsegregational killing does not increase plasmid stability but acts to mediate the exclusion of competing plasmids. *Proceedings of the National Academy of Sciences* 97: 12643–12648.

716 Cooper, T.F., Paixão, T. and Heinemann, J.A. 2010. Within-host competition selects
717 for plasmid-encoded toxin–antitoxin systems. *Proceedings of the Royal*
718 *Society B: Biological Sciences* 277: 3149–3155.
719 Dimitriu, T., Kurilovich, E., Łapińska, U., Severinov, K., Pagliara, S., Szczelkun, M.D.
720 and Westra, E.R. 2022. Bacteriostatic antibiotics promote CRISPR-Cas
721 adaptive immunity by enabling increased spacer acquisition. *Cell Host &*
722 *Microbe* 30: 31-40.e5.
723 Fraikin, N. and Melderen, L.V. 2023. Single-cell evidence for plasmid addiction
724 mediated by toxin-antitoxin systems. 2023.08.29.555305.
725 Fraikin, N. and Van Melderen, L. 2024. Single-cell evidence for plasmid addiction
726 mediated by toxin–antitoxin systems. *Nucleic Acids Research* 52: 1847–1859.
727 Fraikin, N., Couturier, A. and Lesterlin, C. 2024. The winding journey of conjugative
728 plasmids toward a novel host cell. *Current Opinion in Microbiology* 78:
729 102449.
730 Garcillán-Barcia, M.P. and de la Cruz, F. 2008. Why is entry exclusion an essential
731 feature of conjugative plasmids? *Plasmid* 60: 1–18.
732 Georjon, H. and Bernheim, A. 2023. The highly diverse antiphage defence systems
733 of bacteria. *Nature Reviews Microbiology* 21: 686–700.
734 Guan, J., Chen, Y., Goh, Y.-X., Wang, M., Tai, C., Deng, Z., Song, J. and Ou, H.-Y.
735 2024. TADB 3.0: an updated database of bacterial toxin–antitoxin loci and
736 associated mobile genetic elements. *Nucleic Acids Research* 52: D784–D790.
737 Hall, J.P.J., Wright, R.C.T., Guymer, D., Harrison, E. and Brockhurst, M.A. 2019.
738 Extremely fast amelioration of plasmid fitness costs by multiple functionally
739 diverse pathways. *Microbiology* 166.
740 Harms, A., Brodersen, D.E., Mitarai, N. and Gerdes, K. 2018. Toxins, Targets, and
741 Triggers: An Overview of Toxin-Antitoxin Biology. *Molecular Cell* 70: 768–784.
742 Hyatt, D., Chen, G.-L., LoCascio, P.F., Land, M.L., Larimer, F.W. and Hauser, L.J.
743 2010. Prodigal: prokaryotic gene recognition and translation initiation site
744 identification. 11: 119.
745 Igler, C., Huisman, J.S., Siedentop, B., Bonhoeffer, S. and Lehtinen, S. 2021.
746 Plasmid co-infection: linking biological mechanisms to ecological and
747 evolutionary dynamics. *Philosophical Transactions of the Royal Society B:*
748 *Biological Sciences* 377: 20200478.
749 Kippnich, J., Benz, F., Uecker, H. and Baumdicker, F. 2024. Effectiveness of
750 CRISPR-Cas in Sensitizing Bacterial Populations with Plasmid-Encoded
751 Antimicrobial Resistance. 2024.07.05.602127.
752 Klümper, U., Riber, L., Dechesne, A., Sannazzarro, A., Hansen, L.H., Sørensen, S.J.
753 and Smets, B.F. 2015. Broad host range plasmids can invade an
754 unexpectedly diverse fraction of a soil bacterial community. *The ISME Journal*
755 9: 934–945.
756 Kondratyeva, K., Salmon-Divon, M. and Navon-Venezia, S. 2020. Meta-analysis of
757 Pandemic Escherichia coli ST131 Plasmidome Proves Restricted Plasmid-
758 clade Associations. *Scientific Reports* 10: 36.
759 Koonin, E.V. and Makarova, K.S. 2024. CRISPR in mobile genetic elements:
760 counter-defense, inter-element competition and RNA-guided transposition.
761 *BMC Biology* 22: 295.
762 Li, L., Dechesne, A., He, Z., Madsen, J.S., Nesme, J., Sorensen, S.J. and Smets,
763 B.F. 2018. Estimating the Transfer Range of Plasmids Encoding Antimicrobial
764 Resistance in a Wastewater Treatment Plant Microbial Community.
765 acs.estlett.8b00105.

766 Lundquist, P.D. and Levin, B.R. 1986. TRANSITORY DEREPRESSION AND THE
767 MAINTENANCE OF CONJUGATIVE PLASMIDS. *Genetics* 113: 483–497.
768 Mahendra, C., Christie, K.A., Osuna, B.A., Pinilla-Redondo, R., Kleinstiver, B.P. and
769 Bondy-Denomy, J. 2020. Broad-spectrum anti-CRISPR proteins facilitate
770 horizontal gene transfer. *Nature Microbiology* 5: 620–629.
771 Makarova, K.S., Wolf, Y.I., Iranzo, J., Shmakov, S.A., Alkhnbashi, O.S., Brouns,
772 S.J.J., Charpentier, E., Cheng, D., Haft, D.H., Horvath, P., Moineau, S.,
773 Mojica, F.J.M., Scott, D., Shah, S.A., Siksnys, V., Terns, M.P., Venclovas, Č.,
774 White, M.F., Yakunin, A.F., Yan, W., Zhang, F., Garrett, R.A., Backofen, R., van
775 der Oost, J., Barrangou, R. and Koonin, E.V. 2020. Evolutionary classification
776 of CRISPR–Cas systems: a burst of class 2 and derived variants. *Nature*
777 *Reviews Microbiology* 18: 67–83.
778 Martínez-García, E., Calles, B., Arévalo-Rodríguez, M. and de Lorenzo, V. 2011.
779 pBAM1: an all-synthetic genetic tool for analysis and construction of complex
780 bacterial phenotypes. *BMC Microbiology* 11: 38.
781 Mendoza-Suárez, M.A., Geddes, B.A., Sánchez-Cañizares, C., Ramírez-González,
782 R.H., Kirchhelle, C., Jorrin, B. and Poole, P.S. 2020. Optimizing Rhizobium-
783 legume symbioses by simultaneous measurement of rhizobial
784 competitiveness and N2 fixation in nodules. *Proceedings of the National*
785 *Academy of Sciences* 117: 9822–9831.
786 Moya-Beltrán, A., Makarova, K.S., Acuña, L.G., Wolf, Y.I., Covarrubias, P.C.,
787 Shmakov, S.A., Silva, C., Tolstoy, I., Johnson, D.B., Koonin, E.V. and Quatrini,
788 R. 2021. Evolution of Type IV CRISPR-Cas Systems: Insights from CRISPR
789 Loci in Integrative Conjugative Elements of Acidithiobacillia. *The CRISPR*
790 *Journal*.
791 Nazarian, P., Tran, F. and Boedicker, J.Q. 2018. Modeling Multispecies Gene Flow
792 Dynamics Reveals the Unique Roles of Different Horizontal Gene Transfer
793 Mechanisms. 9: 2978.
794 Newire, E., Aydin, A., Juma, S., Enne, V.I. and Roberts, A.P. 2020. Identification of a
795 Type IV-A CRISPR-Cas System Located Exclusively on IncHI1B/IncFIB
796 Plasmids in Enterobacteriaceae. *Frontiers in Microbiology* 11.
797 Novick, R.P. 1987. Plasmid incompatibility. *Microbiological Reviews* 51: 381–395.
798 Pansegrau, W., Lanka, E., Barth, P.T., Figurski, D.H., Guiney, D.G., Haas, D.,
799 Helinski, D.R., Schwab, H., Stanisich, V.A. and Thomas, C.M. 1994. Complete
800 Nucleotide Sequence of Birmingham IncPa Plasmids. *Journal of Molecular*
801 *Biology* 623–663.
802 Patel, P.H. and Maxwell, K.L. 2023. Prophages provide a rich source of antiphage
803 defense systems. *Current Opinion in Microbiology* 73: 102321.
804 Pinilla-Redondo, R., Russel, J., Mayo-Muñoz, D., Shah, S.A., Garrett, R.A., Nesme,
805 J., Madsen, J.S., Fineran, P.C. and Sørensen, S.J. 2022. CRISPR-Cas
806 systems are widespread accessory elements across bacterial and archaeal
807 plasmids. *Nucleic Acids Research* 50: 4315–4328.
808 Prensky, H., Gomez-Simmonds, A., Uhlemann, A. and Lopatkin, A.J. 2021.
809 Conjugation dynamics depend on both the plasmid acquisition cost and the
810 fitness cost. *Molecular Systems Biology* 17.
811 Pursey, E., Sünderhauf, D., Gaze, W.H., Westra, E.R. and van Houte, S. 2018.
812 CRISPR-Cas antimicrobials: Challenges and future prospects. *PLOS*
813 *Pathogens* 14: e1006990.
814 Qiu, D., Damron, F.H., Mima, T., Schweizer, H.P. and Yu, H.D. 2008. PBAD-based
815 shuttle vectors for functional analysis of toxic and highly regulated genes in

Pseudomonas and Burkholderia spp. and other bacteria. *Applied and Environmental Microbiology* 74: 7422–7426.

Rankin, D.J., Turner, L.A., Heinemann, J.A. and Brown, S.P. 2012. The coevolution of toxin and antitoxin genes drives the dynamics of bacterial addiction complexes and intragenomic conflict. *Proceedings of the Royal Society B: Biological Sciences* 279: 3706–3715.

Reuter, A., Hilpert, C., Dedieu-Berne, A., Lematre, S., Gueguen, E., Launay, G., Bigot, S. and Lesterlin, C. 2021. Targeted-antibacterial-plasmids (TAPs) combining conjugation and CRISPR/Cas systems achieve strain-specific antibacterial activity. *Nucleic Acids Research* 49: 3584–3598.

Rocha, E.P.C. and Bikard, D. 2022. Microbial defenses against mobile genetic elements and viruses: Who defends whom from what? *PLOS Biology* 20: e3001514.

Roy, D., Huguet, K.T., Grenier, F. and Burrus, V. 2020. IncC conjugative plasmids and SXT/R391 elements repair double-strand breaks caused by CRISPR–Cas during conjugation. *Nucleic Acids Research* 48: 8815–8827.

San Millan, A. and MacLean, R.C. 2017. Fitness costs of plasmids: a limit to plasmid transmission. *Microbiology Spectrum* 5: 5.5.02.

San Millan, A., Heilbron, K. and MacLean, R.C. 2014. Positive epistasis between co-infecting plasmids promotes plasmid survival in bacterial populations. *The ISME Journal* 8: 601–612.

Sengupta, M. and Austin, S. 2011. Prevalence and Significance of Plasmid Maintenance Functions in the Virulence Plasmids of Pathogenic Bacteria. *Infection and Immunity* 79: 2502–2509.

Siedentop, B., Losa Mediavilla, C., Kouyos, R.D., Bonhoeffer, S. and Chabas, H. 2024. Assessing the Role of Bacterial Innate and Adaptive Immunity as Barriers to Conjugative Plasmids. *Molecular Biology and Evolution* 41: msae207.

Silva-Rocha, R., Martínez-García, E., Calles, B., Chavarría, M., Arce-Rodríguez, A., de las Heras, A., Páez-Espino, A.D., Durante-Rodríguez, G., Kim, J., Nikel, P.I., Platero, R. and de Lorenzo, V. 2013. The Standard European Vector Architecture (SEVA): a coherent platform for the analysis and deployment of complex prokaryotic phenotypes. *Nucleic Acids Research* 41: D666–D675.

Sünderhauf, D., Klümper, U., Gaze, W.H., Westra, E.R. and Van Houte, S. 2023a. Interspecific competition can drive plasmid loss from a focal species in a microbial community. *The ISME Journal*.

Sünderhauf, D., Klümper, U., Pursey, E., Westra, E.R., Gaze, W.H. and van Houte, S. 2023b. Removal of AMR plasmids using a mobile, broad host-range CRISPR-Cas9 delivery tool. *Microbiology* 169: 001334.

Van Sluijs, L., Van Houte, S., Van Der Oost, J., Brouns, S.J., Buckling, A. and Westra, E.R. 2019. Addiction systems antagonize bacterial adaptive immunity. *FEMS Microbiology Letters* 366: 47.

Winter, D.J. 2017. rentrez: An R package for the NCBI eUtils API. *The R Journal* 9: 520–526.

Wu, W.Y., Mohanraju, P., Liao, C., Adiego-Pérez, B., Creutzburg, S.C.A., Makarova, K.S., Keessen, K., Lindeboom, T.A., Khan, T.S., Prinsen, S., Joosten, R., Yan, W.X., Migur, A., Laffeber, C., Scott, D.A., Lebbink, J.H.G., Koonin, E.V., Beisel, C.L. and van der Oost, J. 2022. The miniature CRISPR-Cas12m effector binds DNA to block transcription. *Molecular Cell* 82: 4487-4502.e7.